Surface changes in the eastern Labrador Sea around the onset of the Little Ice Age

Paola Moffa-Sánchez[1], Ian R. Hall[1], Stephen Barker[1], David J. R. Thornalley[1,2], and Igor Yashayaev[3]

[1]School of Earth and Ocean Sciences, Cardiff University, Cardiff, UK, [2]Now at Department of Geography, University College London, London, UK, [3]Ocean Circulation Section, Ocean Sciences Division, Bedford Institute of Oceanography, Fisheries and Oceans Canada, Dartmouth, Nova Scotia, Canada

Abstract Despite the relative climate stability of the present interglacial, it has been punctuated by several centennial-scale climatic oscillations; the latest of which are often colloquially referred to as the Medieval Climatic Anomaly (MCA) and the Little Ice Age (LIA). The most favored explanation for the cause of these anomalies is that they were triggered by variability in solar irradiance and/or volcanic activity and amplified by ocean-atmosphere-sea ice feedbacks. As such, changes in the strength of the Atlantic Meridional Overturning Circulation (AMOC) are widely believed to have been involved in the amplification of such climatic oscillations. The Labrador Sea is a key area of deep water formation. The waters produced here contribute approximately one third of the volume transport of the deep limb of the AMOC and drive changes in the North Atlantic surface hydrography and subpolar gyre circulation. In this study, we present multiproxy reconstructions from a high-resolution marine sediment core located south of Greenland that suggest an increase in the influence of polar waters reaching the Labrador Sea close to MCA-LIA transition. Changes in freshwater forcing may have reduced the formation of Labrador Sea Water and contributed toward the onset of the LIA cooling.

1. Introduction

The Labrador Sea is an active area of formation for the main intermediate water mass of the North Atlantic, known as Labrador Sea Water (LSW). It is one of the few places in the world's oceans where the upper water column during winter can experience complete mixing down to 1.5-2 km [*Lazier et al.*, 2002] and possibly deeper [*Yashayaev*, 2007a]. The formation of deep waters in the Labrador Sea contributes ~30% to the total volume flux of the lower limb of the Atlantic Meridional Overturning Circulation (AMOC) (~15 sverdrup) [e.g., *Rhein et al.*, 2002; *Talley*, 2003]. Specifically, the production and spreading of LSW plays an important role in the AMOC because (i) it influences the properties and volume transport of the Nordic overflows through vigorous entrainment and mixing [e.g., *Price and Baringer*, 1994; *Bersch et al.*, 2007; *Boessenkool et al.*, 2007], (ii) it regulates the surface circulation around the subpolar gyre (SPG) [e.g., *Curry and McCartney*, 2001; *Lu et al.*, 2007], (iii) it fills the intermediate depth reservoir in the North Atlantic, exporting subpolar intermediate waters to the subtropics [*Yashayaev et al.*, 2008; *Bower et al.*, 2009], and (iv) it contributes to the upper component of the dense and deep water masses originating in the Arctic and North Atlantic, collectively termed North Atlantic Deep Water [*Talley and McCartney*, 1982]. Because changes in the AMOC are believed to be a fundamental component of North Atlantic climate variability [*Kuhlbrodt et al.*, 2007], we investigate the potential involvement of LSW formation in centennial-scale climate variability over the past 1200 years.

During wintertime, strong cold westerly winds sweep across the Labrador Sea causing intense heat loss to the atmosphere, which weakens the vertical density gradient and promotes open ocean deep convection, and hence formation of LSW [*Dickson et al.*, 1996; *Marshall and Schott*, 1999; *Yashayaev*, 2007b; *Yashayaev and Loder*, 2009]. The relative strength of the westerlies is often represented by the North Atlantic Oscillation (NAO) index, which is the pressure difference at sea level between the Azores High and the Iceland Low pressure systems [*Hurrell*, 1995]. Deep convection in the Labrador Sea is also controlled by local density gradients, which can be affected by the competing effect of freshwater input from the Arctic Ocean [*Aagaard and Carmack*, 1989; *Dickson et al.*, 2007] and active eddy-driven restratification from Atlantic waters, carried by the northwestern branch of the North Atlantic Current (the Irminger Current) [*Lazier et al.*, 2002; *Straneo*, 2006] and internal SPG circulation [*Yashayaev*, 2007a].

A notable and well-recorded example of the effects of freshwater forcing on deep water formation in the Labrador Sea is the Great Salinity Anomaly (GSA). In 1970, the Labrador Sea received an unusually high discharge of Arctic sea ice and freshwater via the East Greenland Current (EGC), causing a widespread freshening of the upper water column in the North Atlantic [*Dickson et al.*, 1988]. This event was accompanied by a reduction in the depth of winter convection and hence production of LSW [*Lazier*, 1980; *Curry et al.*, 1998]. Coincidentally, the GSA happened during an anomalous negative NAO state between 1968 and 1971. A decrease in the pressure difference between the NAO centers of action (the Icelandic Low and the Azores High) weakened and shifted the positioning of the westerlies, reducing the winter heat loss over the Labrador Sea [*Dickson et al.*, 1996]. During this period the large pressure difference between south Greenland and the Arctic-Asian coast enhanced the transport of Arctic sea ice through Fram Strait, which fed into the EGC and advanced the polar front [*Dickson et al.*, 1988; *Aagaard and Carmack*, 1989; *Walsh and Chapman*, 1990; *Hakkinen*, 1993].

The 1970s GSA is an extraordinary but nonunique event. In the 1990s, a large volume of freshwater from a more local source (Baffin Bay and Labrador Sea) reached the Labrador Sea [*Belkin et al.*, 1998]. However, the large net surface heat loss in the Labrador Sea due to the extreme positive NAO state allowed one of the deepest LSW convection on record [*Lazier et al.*, 2002; *Yashayaev*, 2007b]. The last century has been punctuated by several severe salinity anomalies that have impacted the hydrography of the North Atlantic: 1910, 1970 [*Dickson et al.*, 1988], 1980s [*Belkin et al.*, 1998], and 1990s [*Häkkinen*, 2002; *Belkin*, 2004]. While each differs in origin and nature, they are good examples of the complex interplay between freshwater and atmospheric forcing on LSW convection and its potential alteration of the AMOC [*Gelderloos et al.*, 2012]. However, due to the relatively short time span of instrumental time series, it is difficult to clarify if these anomalies have been a pervasive feature of the North Atlantic climate and if their magnitude and frequency have remained similar throughout the late Holocene.

On centennial time scales, the North Atlantic realm has witnessed several climatic oscillations, the most recent of which are the Medieval Climatic Anomaly (MCA) and the Little Ice Age (LIA). Despite the apparent small-scale climatological changes associated with these periods, they had important socioeconomic and cultural repercussions in Europe and North America [*Lamb*, 1965]. A commonly accepted view on the cause of these anomalies is that they were triggered by an external forcing (either solar and/or volcanic) and amplified by climate feedbacks involving the ocean and the atmosphere [e.g., *Shindell et al.*, 2001; *Goosse et al.*, 2006; *Trouet et al.*, 2009, 2012; *Mignot et al.*, 2011; *Miller et al.*, 2012]. One of the most commonly proposed feedback mechanisms involves changes in sea ice production. A decrease in the radiative forcing during the LIA (increased volcanic activity and/or decreased solar irradiance) would have induced cooling and increased the growth and extent of sea ice in the northern high latitudes, specifically in the Arctic Ocean. The distribution, transport (also affected by changes in atmospheric circulation), and melting of anomalously large amounts of sea ice would have altered the freshwater budget in deep water formation sites, thereby weakening convection and reducing the northward ocean heat transport, which in turn would have reinforced the regional cooling and expansion of sea ice in the high latitudes [*Sedláček and Mysak*, 2009a, 2009b; *Zhong et al.*, 2011; *Miller et al.*, 2012; *Lehner et al.*, 2013]. Other proposed amplifying mechanisms involve changes in atmospheric circulation as a response to solar variability, which would have not only affected the heat transport to Europe but also the ocean circulation in the North Atlantic [*Shindell et al.*, 2001; *Mann et al.*, 2009; *Trouet et al.*, 2009; *Moffa-Sánchez et al.*, 2014].

As described above, changes in North Atlantic circulation, including AMOC variability may have been implicated in these climatic oscillation [*Keigwin*, 1996; *Bianchi and McCave*, 1999; *Bond*, 2001; *Zorita et al.*, 2004; *Sedláček and Mysak*, 2009a; *Thornalley et al.*, 2009; *Hofer et al.*, 2010; *Lehner et al.*, 2013]; however, due to the scarcity of highly resolved marine sedimentary archives, the evidence for centennial-scale changes in AMOC strength is still sparse. Here we present proxy reconstructions with multidecadal temporal resolution from a marine sediment core recovered from south of Greenland spanning the MCA-LIA climate transition. The records show substantial shifts in surface water conditions of the eastern Labrador Sea across the transition, which allow examination of the forcing and variability of the preconditioning of the Labrador Sea for winter convection and its potential role in the AMOC's strength and thus climate over the last millennium.
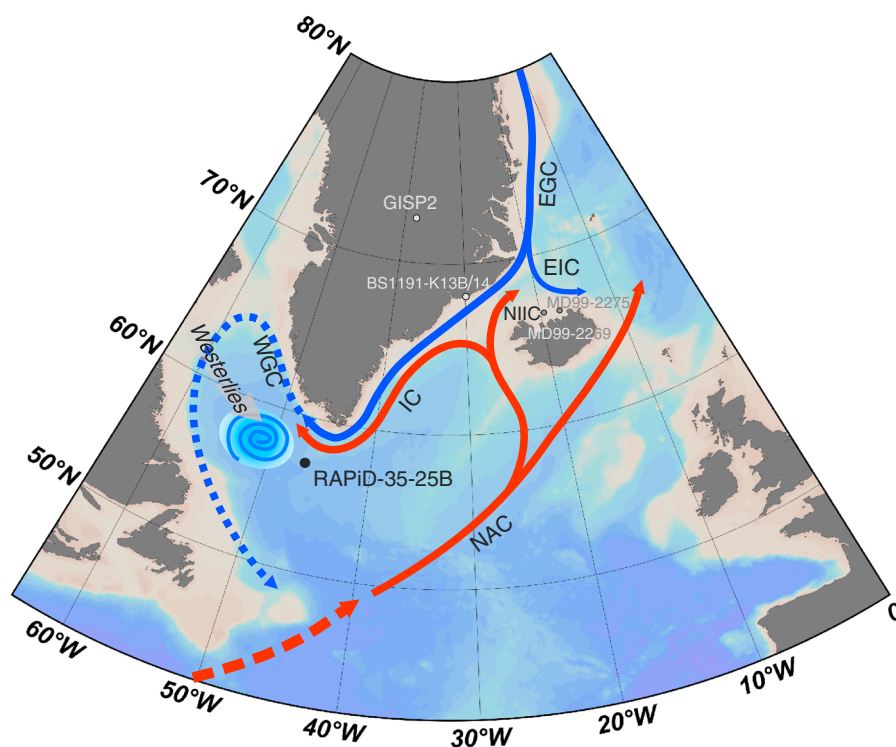
Figure 1. Location map of RAPiD-35-25B. Schematic surface circulation is indicated by the arrows. Blue arrows represent cold polar-derived currents such as the East Greenland Current (EGC) and East Icelandic Current (EIC), and red arrows show Atlantic inflow waters such as North Atlantic Current (NAC), North Icelandic Irminger Current (NIIC), Irminger Current (IC), and West Greenland Current (WGC). The direction of the westerlies is indicated by the gray arrow, and the spiral illustrates the area of deep convection in the Labrador Sea. Locations of published proxy records presented in Figure 6 are indicated in gray.

2. Oceanographic Setting

The eastern sector of the Labrador Sea is a region bathed by mode waters derived from a variety of sources including the Arctic and the Atlantic Oceans [e.g., *Holliday et al.*, 2009]. The EGC is a cold and low-salinity surface ocean current that originates in the Arctic Ocean and flows along the east Greenland continental margin, acting as the main conduit for the export of freshwater into the North Atlantic [*Aagaard and Coachman*, 1968a, 1968b] (Figure 1). Around 70°N a portion of the EGC branches eastward, flowing as the East Icelandic Current (EIC) along the north of Iceland. Periods of increased southward transport of polar waters by the EGC and the EIC increase the export of drift ice and promote colder conditions north of Iceland, a characteristic feature of a southeastward advance of the polar front [*Moros et al.*, 2006].

Once the EGC crosses the Denmark Strait, it encounters Atlantic waters from the Irminger Current (IC), the western branch of the North Atlantic Current (NAC). These two currents form a strong frontal zone, with the IC often underlying the EGC and flow southward to the southern tip of Greenland (Figure 1). Here the boundary currents decelerate and bifurcate with a portion of the EGC and IC entering the deep basin of the Labrador Sea [*Lavender et al.*, 2005; *Holliday et al.*, 2007], while the remaining flow continues northward along the Greenland margin as the West Greenland Current. The temperature and salinity conditions of the EGC and IC, and most importantly their relative contribution to the surface waters of the central Labrador Sea, play a critical role in the process of summer restratification and hence preconditioning of the water column for the following winter's convective activity [*Lazier et al.*, 2002; *Luo et al.*, 2012].

3. Materials and Methodology

3.1. Core Location

Sediment box-core RAPiD-35-25B (57°30.47'N, 48°43.40'W, 3486 m water depth) was recovered from Eirik Drift off the southern tip of Greenland in the eastern sector of the Labrador Sea during the RRS *Charles Darwin*
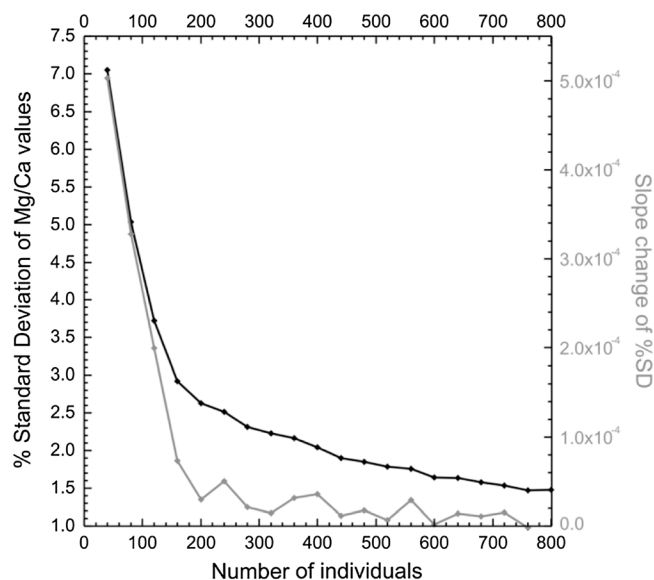
Figure 2. Number of *Nps* individuals picked against percent standard deviation (% SD) of the Mg/Ca values using "jacknife tool." The slope change of the % SD is shown in gray. Dotted line is the % SD from the calculations obtained using a random number generator for grouping the Mg/Ca values.

CD159 cruise (July 2004) (Figure 1). Eirik Drift is a contourite deposit with high sedimentation rates caused by the deposition of sediment that has been eroded from the Denmark Strait and the eastern Greenland margin and transported by the Deep Western Boundary Current (DWBC). As the DWBC turns northward at the south tip of Greenland it decelerates allowing the deposition of the suspended sediment that contribute to the high sediment accumulation rates observed over the Eirik Drift [*Hunter et al.*, 2007a, 2007b]. The high sediment accumulation rates at Eirik Drift (typically 35–200 cm/kyr) have enabled the study of past ocean changes at high temporal resolution by previous investigators [e.g., *Kleiven et al.*, 2008; *Irvali et al.*, 2012].

RAPiD-35-25B was continuously sliced at 0.5 cm intervals, disaggregated on a rotating wheel, and sieved over a 63 μm sieve, and the resulting fine (<63 μm) and coarse (>63 μm) fractions dried at 40°C.

3.2. Planktonic Foraminifera δ^{18}O and Mg/Ca Measurements

We use stable oxygen isotope (δ^{18}O) and Mg/Ca measurements in two species of planktonic foraminifera to reconstruct changes in the surface hydrography of the eastern Labrador Sea over the last millennium. Between 40 and 70 specimens of *Turborotalita quinqueloba* were selected from the 150–212 μm size fraction. Because of their low test weight (~1 μg/test), this species was used solely for stable isotope analysis. Around 180–200 individuals of the polar planktonic foraminifera species *Neogloboquadrina pachyderma* (*sinistral*) (hereinafter *Nps*) were picked from the 150–212 μm size fraction for paired Mg/Ca and δ^{18}O measurements.

A simple experiment was carried out initially to establish the optimal number of *Nps* individuals required to attain Mg/Ca values that were statistically representative of the *Nps* population in our samples. We measured Mg/Ca in 20 subsamples of 40 individuals each from the same interval and conclude that using 160–200 individuals reduces the natural variability in Mg/Ca measurements from a relative standard deviation of 7.2% in 20 individuals to 2.7% (Figure 2). This is similar to the average error of ±4% obtained when measuring duplicates of 20 *Nps* Mg/Ca samples (each containing 150–200 individuals). All analyses were subsequently run using 150–200 individuals.

Stable isotope measurements on the foraminiferal shells were performed on the Thermo Finnigan MAT 252 mass spectrometer coupled to a Kiel II carbonate preparation device at Cardiff University. The spectrometer was calibrated through the international standard NBS-19, and all isotopic results are reported as a per mil deviation from the Vienna Pee Dee Belemnite scale (‰ VPDB). External reproducibility of carbonate standards was 0.08‰ for δ^{18}O.

Samples for paired Mg/Ca and δ^{18}O analysis were prepared and cleaned following the protocol outlined by *Barker et al.* [2003]. The samples were analyzed on the high-resolution inductive coupled plasma mass spectrometry at Cardiff University with an analytical precision for Mg/Ca ratios of better than ±2% relative standard deviation (RSD) and a long-term precision of better than ±2.5% RSD. Average shell weights and comparison of the Mg/Ca record with metals such as Fe, Mn, and Al suggest that secondary effects such as partial dissolution or trace metal contamination have not altered the primary Mg/Ca signal. The Fe/Mg in the *Nps* were mostly found to be below the recommended threshold values by *Barker et al.* [2003] of 0.1 mol/mol and below 0.1 mmol/mol for Al/Ca. Samples between 13 and 15 cm depth presented Fe/Ca values up to

0.23 mmol/mol caused by the presence of pyrite (as recorded by visual inspection), which should not alter the Mg/Ca signal.

Mg/Ca ratios are converted to temperatures using the species-specific calibration equation for *Nps* obtained from a North Atlantic core-top study by *Elderfield and Ganssen* [2000] with the form of

$$Mg/Ca = 0.5 \exp(0.1T) \tag{1}$$

The derived calcification temperatures were used to determine the oxygen isotopic composition of seawater ($\delta^{18}O_{sw}$) by extracting the temperature component from the $\delta^{18}O$ of the calcite using the paleotemperature equation [*Shackleton*, 1974]. In this study, no vital effect correction was applied to the *Nps* $\delta^{18}O$ values, as this factor still remains largely unconstrained in the North Atlantic [*Kohfeld et al.*, 1996; *Nyland et al.*, 2006; *Kozdon et al.*, 2009a; *Jonkers et al.*, 2010] probably because of differences in the regional hydrography and ontogenic effects.

Salinity was estimated following the modern Labrador Sea $\delta^{18}O_{sw}$-salinity relationship from *LeGrande and Schmidt* [2006], and it was assumed that this relationship remained the same down core to enable comparison to modern hydrographic data.

$$Salinity = \left(\delta^{18}O_{sw} - 32.45\right)/0.94 \quad R^2 = 0.87 \tag{2}$$

Core-top temperature and salinity estimates from paired Mg/Ca-$\delta^{18}O$ measurements are comparable to spring/summer modern temperature and salinities at 50–200 m depth (Figures 3e and 3f) (cruise CD159 Conductivity Temperature Depth (CTD) profile and Word Ocean Atlas 2009 data) which is the approximate blooming season [*Jonkers et al.*, 2010] and calcification depth of *Nps* [*Kohfeld et al.*, 1996; *Simstich et al.*, 2003].

For error estimates we used the average error of ±4% RSD from the duplicate measurements of 20 *Nps* Mg/Ca samples and a standard error propagation calculation for a quadratic paleotemperature equation including analytical and calibration errors for paleotemperature and $\delta^{18}O_{sw}$ which are ±0.8°C, ±0.2‰, respectively. Following *Schmidt* [1999] salinity error calculations based on the uncertainties in the relationship between $\delta^{18}O_{sw}$ and salinity, we estimate an error in salinity of ±0.8 practical salinity unit (psu).

3.3. Assemblage Counts

Species composition of planktonic foraminiferal assemblages is sensitive to surface water conditions, specifically sea surface temperatures [*Morey et al.*, 2005]. Such a relationship has been empirically calibrated to enable conversion from census assemblage counts to the reconstruction of past surface water temperatures [*Kucera et al.*, 2005]. Specifically, the percentage of the polar species *Nps* can be used to study past surface temperature variability in the North Atlantic [e.g., *Eynaud*, 2011]. The size fraction 150–250 µm was split to yield a minimum of 350 individuals, and planktonic foraminifera specimens were identified and counted.

4. Core Chronology

In order to provide a chronology, ^{210}Pb dating was carried out in the <63 µm fraction of RAPiD-35-25B, at the University of Sussex, using a Canberra well-type ultralow background hyper pure germanium gamma ray spectrometer to determine the activities of ^{210}Pb and other gamma emitters. Energy and efficiency calibrations were carried out using bentonite clay spiked with a mixed gamma-emitting radionuclide standard, QCYK8163, and checked against a marine sediment reference material (IAEA 135).

The $^{210}Pb_{excess}$ profile presents an exponential decay of unsupported ^{210}Pb down to ~6 cm depth where total ^{210}Pb activities fall to virtually constant background values (Figure 4a), indicating generally low levels of bioturbation and a shallow mixed layer. Sediment accumulation rates were determined by the slope of the least squares fit for the natural log of the $^{210}Pb_{excess}$ activity versus depth. The ^{210}Pb results suggest a sedimentation rate of ~40 cm/kyr for the uppermost 6 cm of the sediment core.

Additionally, seven ^{14}C accelerator mass spectrometer (AMS) dates were measured from monospecific samples of *Nps* (>150 µm) (Table 1). Radiocarbon measurements were made at National Ocean Sciences AMS Facility (NOSAMS-Woods Hole) and the Natural Environment Research Council (NERC) Radiocarbon Laboratory (Table 1). The radiocarbon ages were converted into calendar years using the Marine09 data
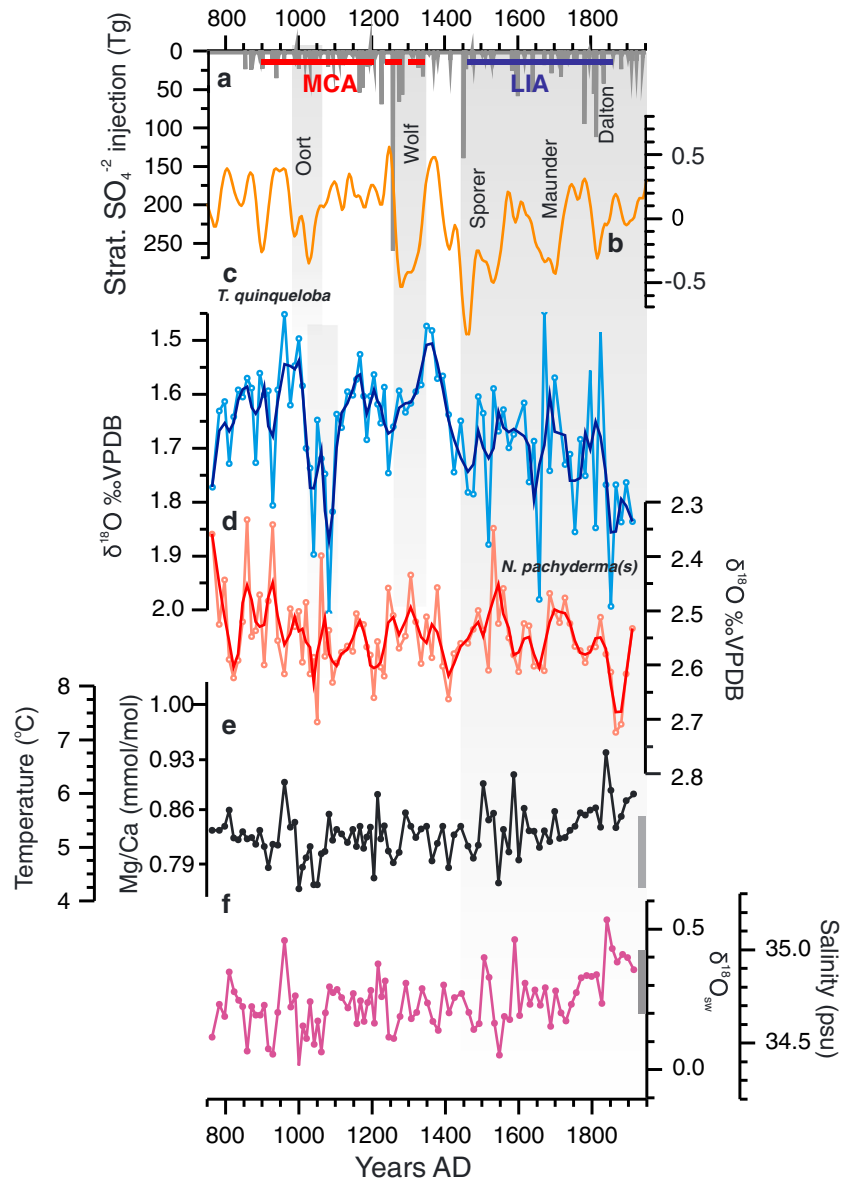
Figure 3. (a) Global stratospheric injection of sulfate (Tg)—proxy for explosive volcanism [*Gao et al.*, 2007], (b) [10]Be-based TSI [*Steinhilber et al.* 2009], and (c) δ^{18}O *T. quinqueloba*. The large shaded area marks the shift in the δ^{18}O *T. quinqueloba* which is coincident with the onset of the LIA. The two shaded bands indicate the periods of solar minima during the MCA. (d–f) *Nps* δ^{18}O, Mg/Ca-based temperature, and $\delta^{18}O_{sw}$ salinity. Gray vertical bars on Figures 3e and 3f are modern annual temperature and salinity ranges (100–200 m depth) at the site from cruise CTD data, *Holliday et al.* [2009], and World Ocean Atlas 2009.

set [*Reimer et al.*, 2009], and the core chronology was constructed using a Bayesian age model software; BChron [*Haslett and Parnell*, 2008; *Parnell et al.*, 2011] (Table 1).

The calibrated ^{14}C dates present a linear distribution down core ($R^2 = 0.98$), suggesting a relatively constant sedimentation rate with an average of ~40 cm/kyr and a sample integration of ~14 years for every 0.5 cm sample (Figure 4b) which is consistent with the sedimentation rate estimated from the ^{210}Pb decay curve.

However, the AMS ^{14}C date at 6.25 cm appears to deviate ~140 years from the linear fit through the other six radiocarbon dates (Figure 4b) and it is also inconsistent with the dating estimate from [210]Pb. The presence of [210]Pb$_{excess}$ at 5 cm depth indicates that the age at 6.25 cm must be younger than ~1780 years A.D. (as no ^{210}Pb would be found beyond 6 times the ^{210}Pb half-life, ~150 years). We therefore consider this ^{14}C date as an outlier and exclude it from the final age model (Figure 4b). A likely explanation for this anomalous date could be a
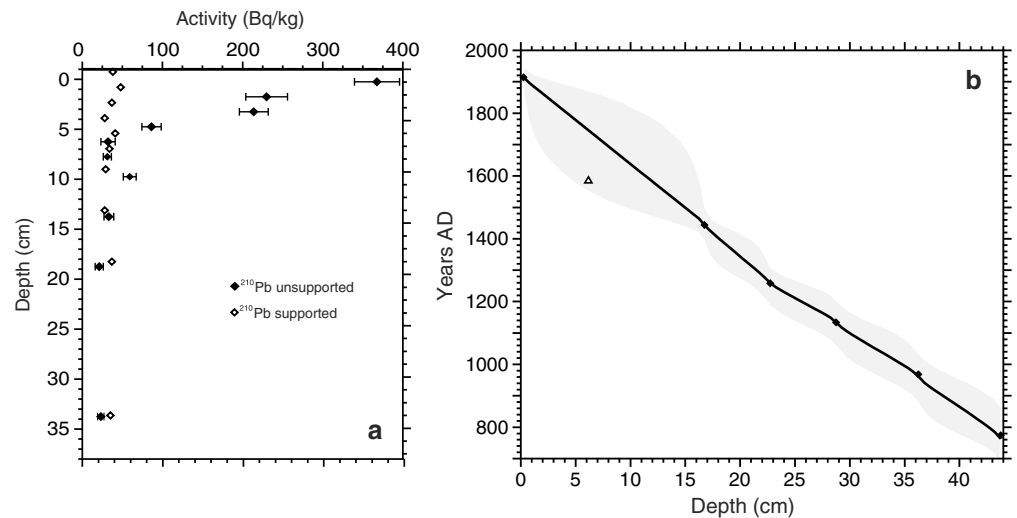
Figure 4. (a) Down-core ^{210}Pb unsupported and supported measurements (filled and empty diamonds, respectively). (b) Core chronology for RAPiD-35-25B based on Bayesian Model run on BChron and based on six radiocarbon dates in black bold line (excluding the date at 6.25 cm highlighted by empty triangle). The shaded area indicates the 95% probability error within the age model calculated in BChron.

change in the regional marine reservoir correction (ΔR) of the waters bathing the site during the LIA as found, for example, in other marine records north of Iceland [*Eiríksson et al.*, 2011; *Wanamaker et al.*, 2012].

5. Results and Discussion

5.1. Surface Water Reconstructions From RAPiD-35-25B

The planktonic foraminifer *T. quinqueloba* is a symbiont-bearing subpolar species which is considered to live in the photic zone, mostly inhabiting the near-surface waters above the summer pycnocline ~50 m at the site [*Tolderlund and Be*, 1971; *Hemleben et al.*, 1989; *Carstens et al.*, 1997; *Simstich et al.*, 2003]. It can therefore be used to monitor a combination of signals indicative of summer restratification processes at the site, including summer warming due to increased seasonal insolation and the influence of fresh and cold water masses such as the EGC and the East Greenland Coastal Current [*Bacon et al.*, 2002; *Holliday et al.*, 2006].

The δ^{18}O record from *T. quinqueloba* in RAPiD-35-25B shows high-amplitude variations of ~0.35‰ between 700 and 1400 years A.D. with a long-term trend of ~0.2‰ toward heavier isotopic values (from 1.65‰ to 1.85‰) from around 1400 years A.D. toward the present (Figure 3c). From 750 to 1400 years A.D. the record shows similar covariability with total solar irradiance (TSI) [*Steinhilber et al.*, 2009] (Figure 3b), particularly during the Oort and Wolf solar minima. This is possibly indicative of irradiance-driven summer temperature variability and enhanced melting of sea ice and the Greenland ice sheet during the warm MCA (Figure 3b). This relationship breaks down, and no covariability is found beyond ~1400 years A.D., when the trend to heavier planktonic δ^{18}O commences (Figures 3b and 3c), perhaps due to a different process dominating the signal discussed below. The heavy δ^{18}O isotopic trend continues until the present without a transition at the end of

Table 1. Radiocarbon Dates Obtained for RAPiD-35-25B

Code[a]	Depth (cm)	Radiocarbon Age ±1σ (Years B.P.)	95% Confidence Age Intervals (Years A.D.)	Calibrated Age (Years A.D.)
OS-82608	0.25	285 ± 30	1942–1877	1914
SUERC-35759	6.25	720 ± 37	1663–1499	1585
OS-86418	16.75	895 ± 25	1483–1399	1444
SUERC-35760	22.75	1145 ± 35	1309–1179	1258
OS-86417	28.75	1270 ± 25	1214–1059	1134
SUERC-35761	36.25	1437 ± 37	1040–867	968
OS-82607	43.5	1610 ± 35	881–696	774

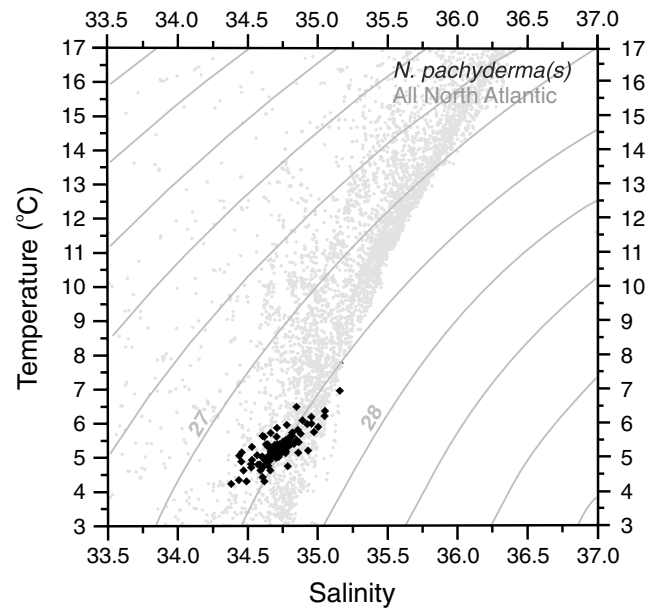[a]OS: NOSAMS and SUERC: NERC radiocarbon facility.

Figure 5. Temperature and salinity diagram. Gray lines indicate lines of same density (isopycnals). The gray points are all of the surface (0–200 m) Global Ocean Data Analysis Project data for the North Atlantic between 30 and 80°N [*Key et al.*, 2004]. The black data points indicate the temperature and salinity values obtained from paired Mg/Ca and $\delta^{18}O$ measurements on *Nps*.

the LIA, which is a common feature observed in other high-resolution subpolar North Atlantic records [*Massé et al.*, 2008; *Kaufman et al.*, 2009; *Richter et al.*, 2009; *Sicre et al.*, 2011] and may have been driven by the precession-derived decline in Northern Hemisphere summer insolation. Some of the observed short-lived excursions to heavier $\delta^{18}O$ values (such as the one at ~1200 years A.D.) coincide with the timing of large volcanic eruptions, as indicated by global stratospheric injection of sulfates [*Gao et al.*, 2007] (Figure 3a), so it is possible that additional cooling from these also left an imprint on the $\delta^{18}O$ record. For instance, the large thirteenth century eruption has been shown in data and models to have caused cooling in the North Atlantic and increased production of sea ice [*Sicre et al.*, 2011; *Zhong et al.*, 2011; *Miller et al.*, 2012].

Nps also lives in the surface waters, although it typically calcifies deeper down in the water column giving an approximate signal of ~100–200 m depth [*Stangeew*, 2001; *Simstich et al.*, 2003; *Kozdon et al.*, 2009b]. The $\delta^{18}O$ *Nps* record shows relative stability, with only slight centennial-scale amplitude changes and a maximum variability of ~0.2‰ over the last 1200 years (Figure 3d). Similarly, paired Mg/Ca-$\delta^{18}O$ temperature and salinity reconstructions also suggest stable calcification conditions with a maximum variability of 2°C and 1 psu, respectively, and a slight increase from 1550 years A.D. onward (Figures 3e and 3f). Estimates of density based on the temperature and salinity reconstructions from *Nps* range between approximately 27.5 and 27.8 kg m^{-3} (Figure 5). This is in agreement with previous studies from the Nordic Seas [*Simstich et al.*, 2003; *Kozdon et al.*, 2009b], suggesting that the calcification depth of *Nps* is bound to 27.7 to 27.8 kg m^{-3} isopycnal surfaces.

The difference between $\delta^{18}O$ values of foraminifera that live in different habitat depths is often used to provide information on the stratification of the water column [e.g., *Mulitza et al.*, 1997; *Rashid and Boyle*, 2007]. In particular, a study of the $\delta^{18}O$ difference between *T. quinqueloba* and *Nps* in the Nordic Seas concluded that the difference can provide information on the thermal stratification of the water column [*Simstich et al.*, 2003]. The largest offset in $\delta^{18}O$ between the two species was found in regions that are influenced by Atlantic waters from the IC [*Simstich et al.*, 2003]. In RAPiD-35-25B we observe a larger average difference between the $\delta^{18}O$ of *T. quinqueloba* and *Nps* from the period 750–1400 years A.D. (~0.95‰) which respect to the 1400–1960 years A.D. (~0.85‰) (Figures 3c and 3d). In the period from 1400 years A.D. toward present there is a coherent variability of $\delta^{18}O$ between the two species (Figures 3c and 3d). This feature could suggest increased upper column thermal stratification, indicative of a larger influence of Atlantic versus polar waters reaching the site via the IC, before ~1400 years A.D. However, we note a recent sediment trap study by *Jonkers et al.* [2010] in the Irminger Sea suggests that *T. quinqueloba* and *Nps* show seasonal differences in the timing of their blooms. Thus, the large differences in $\delta^{18}O$ during 750–1400 years A.D. could also indicate changes in the seasonal thermal contrast, for instance warmer summers (*T quinqueloba* blooming time) with respect to spring (*Nps* blooming time).

5.2. Cold Conditions in the Surface Labrador Sea at the Onset of the LIA

Surface water density changes can have a strong influence on the degree of deep convection in the Labrador Sea and are often a consequence of the interplay between variable freshwater input, advection of salt and heat within the IC and heat loss from wind stress forcing. The shallow depth habitat of *T. quinqueloba* makes it a potentially sensitive indicator of hydrographic changes in the surface eastern Labrador Sea. However, the

δ^{18}O record of *T. quinqueloba* contains both a temperature and δ^{18}O$_{sw}$ component and it is hard to disentangle the contribution of these properties to the signal without an additional independent temperature proxy. In order to tackle this issue hydrographic temperature and salinity measurements from the Labrador Sea (section AR7W) [see *Yashayaev*, 2007a, Figure 1] for the last 60 years were used to estimate the ambient δ^{18}O of the seawater and thus predict the δ^{18}O calcite (δ^{18}O$_{predicted}$) that would be recorded by *T. quinqueloba* (assuming no vital effects). Annual summer time average surface (0–30 m) temperature and salinity measurements over the last 60 years from the Labrador Sea show a positive linear relationship ($R^2 = 0.70$, Figures S1a and S1b in the supporting information). δ^{18}O$_{predicted}$ shows a strong negative relationship with temperature ($R^2 = 0.64$, Figure S1c), as would be expected if temperature were the dominant control on δ^{18}O$_{predicted}$ (if salinity were the dominant signal we would expect to observe a positive relationship between salinity and δ^{18}O$_{predicted}$). Therefore, based on the magnitude of typical temperature and salinity changes in the modern surface Labrador Sea over the last 60 years, we conclude that the δ^{18}O signal from *T. quinqueloba* in RAPiD-35-25B is likely to have been dominated by changes in sea surface temperature. Assuming that the ~0.25‰ change in the δ^{18}O of *T. quinqueloba* (Figure 6f) at ~1400 years A.D. and the average shift of ~0.08‰ before and after ~1400 years (dotted line in Figure 6f) were driven by temperature changes alone, we predict (from the modern δ^{18}O$_{predicted}$-temperature relationship) a maximum cooling of ~2.5°C and ~1°C, respectively. The transition to colder surface temperatures at ~1400 years A.D. is supported by the faunal assemblage changes (Figure 6g), which provide an independent quantitative ecological parameter. The relative percentage of the polar species *Nps* can be used to monitor past temperatures at the site and the relative influence of polar waters [*Hilbrecht*, 1997]. Assemblage counts on RAPiD-35-25B reveal abrupt shifts in *Nps* of ~35% during the period between 700 and 1400 years A.D. (Figure 6g) with a transition at ~1400 years A.D. from a mean of ~76% *Nps* to an increased presence of *Nps* to about ~85%, which continues until the present (Figure 6g). Using transfer function and modern *Nps* distribution studies [*Hilbrecht*, 1996, 1997; *Kucera*, 2007; *Eynaud*, 2011], this shift in percent abundance of *Nps* equates to a temperature shift of ~1.5°C, similar to the estimated temperature changes contributing to the predicted temperature from the δ^{18}O values from *T. quinqueloba* at the MCA-LIA transition (Figure 6f).

The recorded surface cooling in the Labrador Sea at ~1400 years A.D. could be explained by either (i) an increase in the influence of cold and fresh polar waters from the EGC or (ii) an invigoration of the winter convection via wind stress forcing during severe winters which would have eroded the surface layer bringing colder waters to the surface. To help discriminate between these two mechanisms; freshwater or wind stress forcing, we compare our results with other ocean and atmospheric proxy records (Figure 6).

5.3. The Onset of the Little Ice Age: A Shift in Atmosphere-Ocean Conditions

Documentary archives suggest that during periods of the MCA, large parts of the coast of Greenland were ice free. Conversely, recurrent invasions of drift ice sourced from the Arctic Ocean were documented to have reached the North Icelandic Shelf during the LIA [*Koch*, 1945; *Ogilvie and Jónsson*, 2001] (Figure 6d). Naturally, some caution is needed when using Icelandic documentary sources to monitor southerly advances of the polar front because (i) these may underrepresent more intermediate advances and (ii) the documentary evidence for the presence of Icelandic drift ice is more fragmentary before 1600 years A.D. (Figure 6d). The timing and magnitude of a southward shift of the polar front and the greater influence of polar waters reaching the Denmark Strait, and very likely extending to the Labrador Sea, have also been recorded in several proxy records over the last millennium. The organic geochemistry sea ice proxy IP25 [*Belt et al.*, 2007; *Massé et al.*, 2008] records fluctuations in the presence of sea ice conditions north of Iceland which are directly comparable to the observations documented by *Ogilvie and Jónsson* [2001] (Figures 6d and 6e). The presence of quartz in the North Icelandic Shelf sediments has been shown to indicate the influence of drift ice transported by the EIC [e.g., *Andrews*, 2009] and demonstrates a steady increase in drift ice reaching the coast of North Iceland since ~1000 years A.D. [*Moros et al.*, 2006] (Figure 6c). A transition to colder conditions at ~1400 years A.D. is also observed in diatom assemblages and alkenone-based sea surface temperature reconstructions from the north of Iceland [*Jiang et al.*, 2005; *Sicre et al.*, 2008], which implies a greater influence of polar versus Atlantic waters during the LIA, as also shown in the radiocarbon reservoir ages from absolutely dated bivalves recovered from the same region [*Wanamaker et al.*, 2012]. Additionally, foraminiferal assemblage records from farther south in the Denmark Strait and west Greenland also show an increased influence of polar waters in the EGC and West Greenland Current toward the onset of the LIA [*Jennings and Weiner*, 1996; *Perner et al.*, 2011] (Figure 6c). In summary, there is substantial evidence to
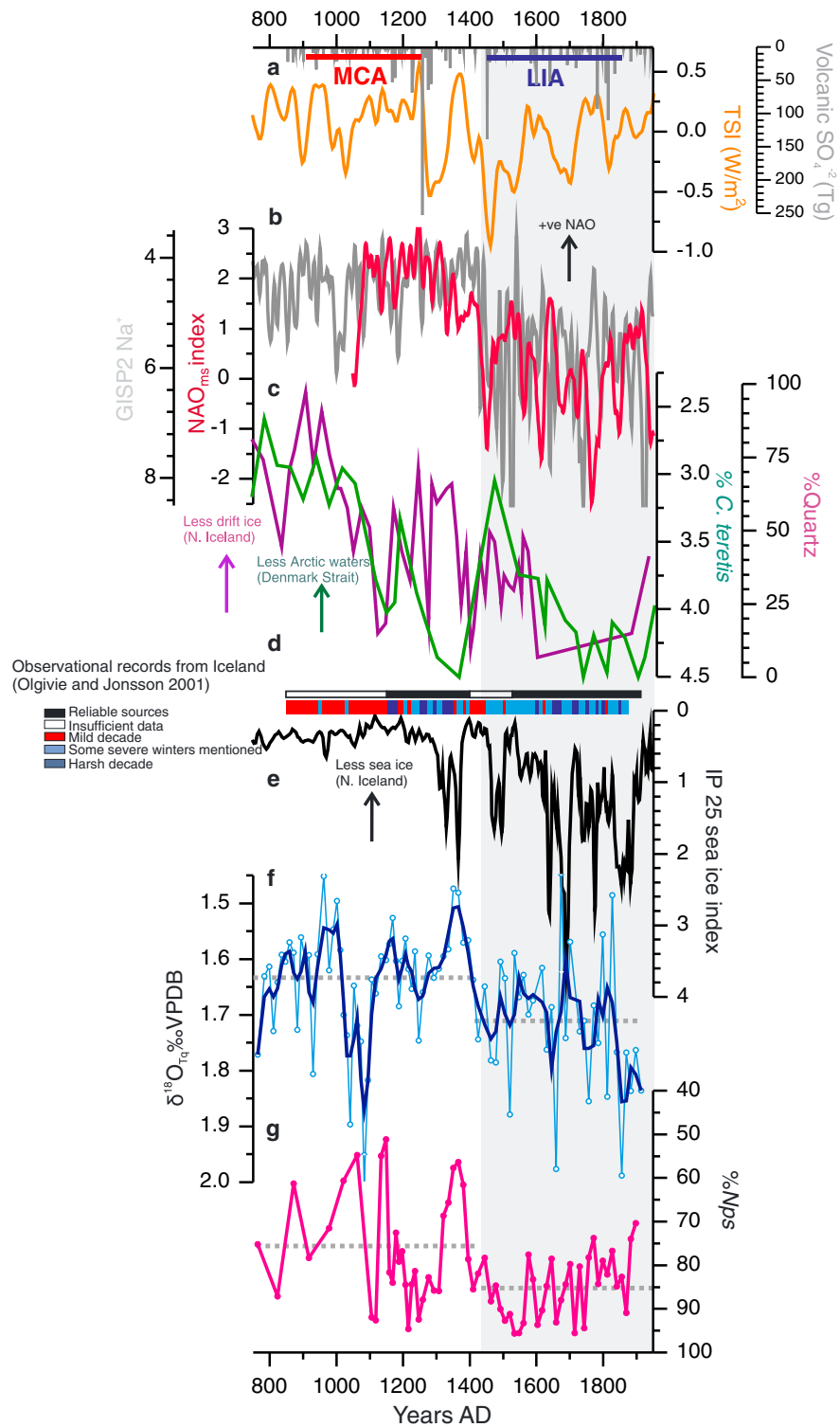
Figure 6. (a) External forcings: volcanic [*Gao et al.*, 2007] (grey) and TSI forcing [*Steinhilber et al.*, 2009] (orange). (b) Atmospheric forcing: Na + concentration in GISP2 [*Mayewski et al.*, 1997] (light grey) and NAO proxy reconstruction [*Trouet et al.*, 2009] (red). (c) Percent quartz from MD99-2269 reaching the North Icelandic Shelf [*Moros et al.*, 2006] (purple) and percent *C. teretis* from BS1191-K13B/14 in the East Greenland Continental Shelf close to the Denmark Strait [*Jennings and Weiner*, 1996] (green). (d) Observational historical records around the Iceland coast [*Ogilvie and Jónsson*, 2001]. (e) IP25 sea ice proxy from MD99-2275 (North Iceland) [*Massé et al.*, 2008]. (f and g) $\delta^{18}O$ from *T. quinqueloba* and percent *Nps*, respectively, from RAPiD-35-25B (this study). The grey shaded area marks the shift at ~1450 years A.D. observed in the majority of the proxies. For location of these proxy reconstructions see Figure 1. The discontinued lines in Figures 6f and 6g indicate the average values before and after 1400 years A.D.

suggest a greater presence of polar waters and drift ice being transported southward via the EGC at the onset of the LIA, which led to the surface cooling recorded at the RAPiD-35-35B site in the eastern Labrador Sea (Figures 6f and 6g). An increase in the cold and fresh polar waters reaching the Labrador Sea would likely have reduced deep convection.

Based on modern observations, the heat loss that leads to winter convection in the Labrador Sea is strongly dependent on the strength of the westerlies [e.g., *Yashayaev*, 2007b]. North Atlantic high-resolution atmospheric records that span the entirety of the last millennium are scarce but increasing in number. One of the earliest attempts to reconstruct North Atlantic atmospheric changes used the sea salt concentration (Na$^+$) in the Greenland Ice Sheet Project 2 (GISP2) as an indication of storminess over Greenland [*Kreutz et al.*, 1997; *Mayewski et al.*, 1997]. This record showed a shift to stormier conditions ~1400 years A.D. which was associated with changes toward positive NAO conditions [*Meeker and Mayewski*, 2002; *Dawson et al.*, 2007]. Numerous terrestrial proxy records from around the North Atlantic, particularly NW Europe, are consistent in showing an increase in the storminess at the onset of the LIA, which has often been related to more positive NAO-like conditions [e.g., *Wintle et al.*, 1998; *de Jong et al.*, 2006; *Nesje et al.*, 2008; *De Jong et al.*, 2009].

However, *Trouet et al.* [2009] utilized a tree ring drought record from Morocco (2009) and a speleothem-based precipitation record from NW Scotland [*Proctor et al.*, 2000] to produce an NAO reconstruction extending back 1000 years. The results show evidence for persistent positive NAO-like atmospheric conditions during the MCA which transitioned toward more negative conditions at the onset of the LIA [*Trouet et al.*, 2009] (Figure 6b). Recent paleoenvironmental reconstructions from Morocco [*Wassenburg et al.*, 2013], the Iberian Peninsula [*Abrantes et al.*, 2011; *Moreno et al.*, 2012], Greenland [*Olsen et al.*, 2012], and west U.S. [*D'Arrigo et al.*, 2012] are also consistent and further confirm that the MCA was likely a period dominated by a positive NAO state compared to the LIA, although with perhaps more variability than initially suggested [*Lehner et al.*, 2012; *Olsen et al.*, 2012; *Wassenburg et al.*, 2013].

As summarized above, the majority of atmospheric proxy studies are consistent in recording changes in the North Atlantic atmospheric circulation around the onset of the LIA (Figure 6b), although there is disagreement with the interpretation between records as to whether this shift was a transition toward a positive [e.g., *Trouet et al.*, 2009] or a negative NAO-like state [e.g., *Meeker and Mayewski*, 2002]. A possible explanation for this discrepancy has been provided by *Trouet et al.* [2012], based on *Raible et al.* [2007], who argue that the increase in storminess during the LIA was not due to an increase in the frequency of storms associated with a positive NAO but more likely that these storms were more intense during the LIA. Numerous modeling studies support the notion of the LIA being a period of more negative NAO-like atmospheric circulation compared to the MCA mainly as a response of the atmosphere to the changes in solar irradiance [e.g., *Shindell et al.*, 2001; *Mann et al.*, 2009; *Spangehl et al.*, 2010; *Swingedouw et al.*, 2011], a relationship that has also been found in the observational record at decadal time scales [*Barriopedro et al.*, 2008; *Lockwood et al.*, 2010; *Woollings et al.*, 2010].

Assuming that the MCA-LIA was a transition toward a negative NAO, a weakening of the westerlies would have reduced the heat loss over the Labrador Sea, decreasing the extent of convection. It may also have been a similar atmospheric setup to that of the 1970s in which a strengthening of the Greenland High (during an extreme negative NAO) promoted the southward export of polar waters and Arctic drift ice through the Fram Strait into the Labrador Sea [*Dickson et al.*, 1988; *Walsh and Chapman*, 1990]. However, it is also possible that the strength of the wind stress forcing may have played a minor role compared to the freshwater forcing, similar to the 1980s' salinity anomaly, when the Labrador Sea received a large volume of freshwater and, despite a strong positive NAO state, the wind stress was not enough to remove the surface buoyancy created by the freshwater layer, and hence, LSW production was suppressed [*Belkin et al.*, 1998].

We conclude that the shift to cold ocean conditions recorded in RAPiD-35-25B at the onset of the LIA was very likely caused by an increase in the presence of cold, low-salinity polar waters which may have reduced deepwater convection in the Labrador Sea. It is also possible that a change from a prevalent positive to negative NAO-like state at the MCA-LIA transition may have helped reduced the formation of LSW.

5.4. External Forcings and the MCA-LIA Transition

The ocean changes recorded in the southeast Greenland around the onset of the LIA (Figures 6f and 6g) could have been forced by the decrease in solar irradiance and increase in the frequency and magnitude of explosive

volcanic activity (Figure 6a). Solar irradiance has often been put forward as the driver for changes in the patterns of atmospheric circulation over the North Atlantic. The transition between the MCA and the LIA was also associated with a shift to a higher frequency of solar minima periods (Figure 6a). A number of model studies suggest a negative NAO state during periods of solar minima, specifically the Maunder Minimum [*Shindell et al.*, 2001; *Zorita et al.*, 2004; *Raible et al.*, 2007; *Mann et al.*, 2009; *Spangehl et al.*, 2010]. The relationship between solar activity and atmospheric circulation is frequently explained by stratospheric feedbacks possibly as a response of ozone formation to changes in ultra violet radiation [*Haigh*, 1994; *Shindell et al.*, 2001; *Gray et al.*, 2010; *Haigh et al.*, 2010; *Woollings et al.*, 2010]. Nonetheless, a lot of uncertainty remains and modeling studies with a simplified representation of the upper atmosphere find a similar response to solar forcing, which suggests that other feedback such as upper atmosphere dynamics [*Spangehl et al.*, 2010], Pacific teleconnections [*Mann et al.*, 2005; *Graham et al.*, 2007; *Ineson and Scaife*, 2009; *Swingedouw et al.*, 2011], and perhaps ocean forcing on atmospheric dynamics [*Rodwell et al.*, 1999; *Czaja and Frankignoul*, 2002; *Scaife et al.*, 2013] may also play an important role in the response of the North Atlantic atmospheric circulation to solar irradiance variability.

Additionally, volcanic reconstructions reveal that the frequency and magnitude of volcanic eruptions increased at ~1250 years A.D. (the end of the MCA) [*Gao et al.*, 2007] (Figure 6a). Explosive volcanism has immediate impacts on global surface climate as it exerts a negative radiative forcing, inducing surface cooling [*Bradley*, 1988; *Robock*, 2000; *Sedláček and Mysak*, 2009a]. Despite the short residence time of aerosols in the stratosphere, volcanic eruptions can have longer-lived climatic impacts through sustained ocean-atmospheric feedback [*Schneider et al.*, 2009] such as sea ice [*Zhong et al.*, 2011; *Miller et al.*, 2012]. However, the similar timing of the periods of increased solar minima and volcanic activity have made the separation of their relative influence to the climate of the last millennium difficult [*International Panel on Climate Change*, 2007].

6. Conclusions

We have presented multidecadally resolved proxy reconstructions of the surface eastern Labrador Sea spanning the last millennium. The results record a cooling at ~1400 years A.D., which corresponds to the start of the LIA. From a comparison with other ocean and atmospheric records, we conclude that the onset of cold conditions in the Labrador Sea likely resulted from an increase in the influence of polar waters and perhaps a concomitant shift to a prevalent negative NAO-like pattern. These changes in buoyancy and wind stress forcing, perhaps driven by increased frequency and magnitude of solar minima and explosive volcanism, likely reduced deep convection in the Labrador Sea during the LIA. Future work is necessary to confirm and quantify the effects that the proposed reduction in deepwater formation would have had on the strength of the AMOC and its potential contribution toward the cooling experienced in Europe during the LIA. In light of future alterations in the North Atlantic's freshwater budget from melting of Arctic sea ice and the Greenland ice sheet, it is essential to improve our understanding of the AMOC natural variability and particularly its response to freshwater forcing in the past.

References

Aagaard, K., and E. C. Carmack (1989), The role of sea ice and other fresh water in the arctic circulation, *J. Geophys. Res.*, *94*(C10), 14,485–14,498, doi:10.1029/JC094iC10p14485.
Aagaard, K., and L. Coachman (1968a), The East Greenland Current north of Denmark Strait: Part II, *Arctic*, *21*(4), 267–290.
Aagaard, K., and L. K. Coachman (1968b), The East Greenland Current north of Denmark Strait: Part I, *Arctic*, *21*(3), 181–200.
Abrantes, R. T., B. Montanari, C. Santos, L. Witt, C. Lopes, and A. H. L. Voelker (2011), Climate of the last millennium at the southern pole of the North Atlantic Oscillation: An inner-shelf sediment record of flooding and upwelling, *Clim. Res.*, *48*(2–3), 261–280, doi:10.3354/cr01010.
Andrews, J. T. (2009), Seeking a Holocene drift ice proxy: Non-clay mineral variations from the SW to N-central Iceland shelf: Trends, regime shifts, and periodicities, *J. Quat. Sci.*, *24*(7), 664–676, doi:10.1002/jqs.1257.
Bacon, S., G. Reverdin, I. G. Rigor, and H. M. Snaith (2002), A freshwater jet on the East Greenland shelf, *J. Geophys. Res.*, *107*(C7), 3068, doi:10.1029/2001JC000935.
Barker, S., M. Greaves, and H. Elderfield (2003), A study of cleaning procedures used for foraminiferal Mg/Ca paleothermometry, *Geochem Geophys Geosyst*, *4*(9), 8407, doi:10.1029/2003GC000559.
Barriopedro, D., R. García-Herrera, and R. Huth (2008), Solar modulation of Northern Hemisphere winter blocking, *J. Geophys. Res.*, *113*, D14118, doi:10.1029/2008JD009789.
Belkin, I. M. (2004), Propagation of the Great Salinity Anomaly of the 1990s around the northern North Atlantic, *Geophys Res Lett*, *31*, L08306, doi:10.1029/2003GL019334.
Belkin, I. M., S. Levitus, J. Antonov, and S.-A. Malmberg (1998), "Great Salinity Anomalies" in the North Atlantic, *Prog. Oceanogr.*, *41*(1), 1–68, doi:10.1016/s0079-6611(98)00015-9.
Belt, S. T., G. Massé, S. J. Rowland, M. Poulin, C. Michel, and B. LeBlanc (2007), A novel chemical fossil of palaeo sea ice: IP25, *Org. Geochem.*, *38*(1), 16–27, doi:10.1016/j.orggeochem.2006.09.013.

Bersch, M., I. Yashayaev, and K. P. Koltermann (2007), Recent changes of the thermohaline circulation in the subpolar North Atlantic, *Ocean Dyn.*, *57*(3), 223–235, doi:10.1007/s10236-007-0104-7.

Bianchi, G. G., and I. N. McCave (1999), Holocene periodicity in North Atlantic climate and deep-ocean flow south of Iceland, *Nature*, *397*, 515–517, doi:10.1038/17362.

Boessenkool, K. P., I. R. Hall, H. Elderfield, and I. Yashayaev (2007), North Atlantic climate and deep-ocean flow speed changes during the last 230 years, *Geophys. Res. Lett.*, *34*, L13614, doi:10.1029/2007GL030285.

Bond, G. (2001), Persistent solar influence on north Atlantic climate during the Holocene, *Science*, *294*, 2130–2136, doi:10.1126/science.1065680.

Bower, A. S., M. S. Lozier, S. F. Gary, and C. W. Böning (2009), Interior pathways of the North Atlantic meridional overturning circulation, *Nature*, *459*(7244), 243–247, doi:10.1038/nature07979.

Bradley, R. S. (1988), The explosive volcanic eruption signal in Northern Hemisphere continental temperature records, *Clim. Change*, *12*(3), 221–243, doi:10.1007/BF00139431.

Carstens, J., D. Hebbeln, and G. Wefer (1997), Distribution of planktic foraminifera at the ice margin in the Arctic (Fram Strait), *Mar. Micropaleontol.*, *29*(3–4), 257–269, doi:10.1016/s0377-8398(96)00014-x.

Curry, R. G., and M. S. McCartney (2001), Ocean gyre circulation changes associated with the North Atlantic Oscillation, *J. Phys. Oceanogr.*, *31*(12), 3374–3400.

Curry, R. G., M. S. McCartney, and T. M. Joyce (1998), Oceanic transport of subpolar climate signals to mid-depth subtropical waters, *Nature*, *391*(6667), 575–577, doi:10.1038/35356.

Czaja, A., and C. Frankignoul (2002), Observed impact of Atlantic SST anomalies on the North Atlantic Oscillation, *J. Clim.*, *15*(6), 606–623, doi:10.1175/JCLI3523.1.

D'Arrigo, R., K. J. Anchukaitis, B. Buckley, E. Cook, and R. Wilson (2012), Regional climatic and North Atlantic Oscillation signatures in West Virginia red cedar over the past millennium, *Global Planet. Change*, *84–85*(0), 8–13, doi:10.1016/j.gloplacha.2011.07.003.

Dawson, A. G., K. Hickey, P. A. Mayewski, and A. Nesje (2007), Greenland (GISP2) ice core and historical indicators of complex North Atlantic climate changes during the fourteenth century, *Holocene*, *17*(4), 427–434, doi:10.1177/0959683607077010.

de Jong, R., S. Björck, L. Björkman, and L. B. Clemmensen (2006), Storminess variation during the last 6500 years as reconstructed from an ombrotrophic peat bog in Halland, southwest Sweden, *J. Quat. Sci.*, *21*(8), 905–919, doi:10.1002/jqs.1011.

De Jong, R., D. Hammarlund, and A. Nesje (2009), Late Holocene effective precipitation variations in the maritime regions of south-west Scandinavia, *Quat. Sci. Rev.*, *28*(1–2), 54–64, doi:10.1016/j.quascirev.2008.09.014.

Dickson, R. R., J. Meincke, S. A. Malmberg, and A. J. Lee (1988), The "great salinity anomaly" in the Northern North Atlantic 1968–1982, *Prog. Oceanogr.*, *20*(2), 103–151, doi:10.1016/0079-6611(88)90049-3.

Dickson, R., J. Lazier, J. Meincke, P. Rhines, and J. Swift (1996), Long-term coordinated changes in the convective activity of the North Atlantic, *Prog. Oceanogr.*, *38*, 241–295, doi:10.1016/S0079-6611(97)00002-5.

Dickson, R., B. Rudels, S. Dye, M. Karcher, J. Meincke, and I. Yashayaev (2007), Current estimates of freshwater flux through Arctic and subarctic seas, *Prog. Oceanogr.*, *73*(3–4), 210–230, doi:10.1016/j.pocean.2006.12.003.

Eiríksson, J., K. L. Knudsen, G. Larsen, J. Olsen, J. Heinemeier, H. B. Bartels-Jónsdóttir, H. Jiang, L. Ran, and L. A. Símonarson (2011), Coupling of palaeoceanographic shifts and changes in marine reservoir ages off North Iceland through the last millennium, *Palaeogeogr. Palaeoclimatol. Palaeoecol.*, *302*(1), 95–108, doi:10.1016/j.palaeo.2010.06.002.

Elderfield, H., and G. Ganssen (2000), Past temperature and δ18O of surface ocean waters inferred from foraminiferal Mg/Ca ratios, *Nature*, *405*(6785), 442–445, doi:10.1038/35013033.

Eynaud, F. (2011), Planktonic foraminifera in the Arctic: Potentials and issues regarding modern and quaternary populations, *IOP Conf. Ser. Earth Environ. Sci.*, *14*(1), 012,005, doi:10.1088/1755-1315/14/1/012005.

Gao, C., L. Oman, A. Robock, and G. L. Stenchikov (2007), Atmospheric volcanic loading derived from bipolar ice cores: Accounting for the spatial distribution of volcanic deposition, *J. Geophys. Res.*, *112*, D23111, doi:10.1029/2006JD007461.

Gelderloos, R., F. Straneo, and C. A. Katsman (2012), Mechanisms behind the temporary shutdown of deep convection in the Labrador Sea: Lessons from the Great Salinity Anomaly years 1968–71, *J. Clim.*, *25*(19), 6743–6755, doi:10.1175/JCLI-D-11-00549.1.

Goosse, H., O. Arzel, J. Luterbacher, M. E. Mann, H. Renssen, N. Riedwyl, A. Timmermann, E. Xoplaki, and H. Wanner (2006), The origin of the European "Medieval Warm Period," *Clim. Past Discuss.*, *2*(3), 285–314, doi:10.5194/cp-2-99-2006.

Graham, N. E., et al. (2007), Tropical Pacific—Midlatitude teleconnections in medieval times, *Clim. Change*, *83*(1–2), 241–285, doi:10.1007/s10584-007-9239-2.

Gray, L. J., et al. (2010), Solar influences on climate, *Rev. Geophys.*, *48*, RG4001, doi:10.1029/2009RG000282.

Haigh, J. D. (1994), The role of stratospheric ozone in modulating the solar radiative forcing of climate, *Nature*, *370*(6490), 544–546, doi:10.1038/370544a0.

Haigh, J. D., A. R. Winning, R. Toumi, and J. W. Harder (2010), An influence of solar spectral variations on radiative forcing of climate, *Nature*, *467*(7316), 696–699, doi:10.1038/nature09426.

Hakkinen, S. (1993), An Arctic source for the Great Salinity Anomaly: A simulation of the Arctic ice-ocean system for 1955–1975, *J. Geophys. Res.*, *98*(C9), 16,397–16,410, doi:10.1029/93JC01504.

Häkkinen, S. (2002), Freshening of the Labrador Sea surface waters in the 1990s: Another great salinity anomaly?, *Geophys. Res. Lett.*, *29*(24), 2232, doi:10.1029/2002GL015243.

Haslett, J., and A. Parnell (2008), A simple monotone process with application to radiocarbon-dated depth chronologies, *J. R. Stat. Soc. Ser. C Appl. Stat.*, *57*(4), 399–418, doi:10.1111/j.1467-9876.2008.00623.x.

Hemleben, C., M. Spindler, and R. Anderson (1989), *Modern Planktonic Foraminifera*, Springer, New York.

Hilbrecht, H. (1996), *Extant Planktic Foraminifera and the Physical Environment in the Atlantic and Indian Oceans*, edited by N. F. Mitteilungen aus dem Geologischen Institut der Eidgen, Technischen Hochschule und der Universität, Zürich.

Hilbrecht, H. (1997), Morphologic gradation and ecology in Neogloboquadrina pachyderma and N. dutertrei (planktic foraminifera) from core top sediments, *Mar. Micropaleontol.*, *31*(1–2), 31–43, doi:10.1016/S0377-8398(96)00054-0.

Hofer, D., C. C. Raible, and T. F. Stocker (2010), Variations of the Atlantic meridional overturning circulation in control and transient simulations of the last millennium, *Clim. Past Discuss.*, *6*(4), 1267–1309, doi:10.5194/cpd-6-1267-2010.

Holliday, N. P., J. J. Waniek, R. Davidson, D. Wilson, L. Brown, R. Sanders, R. T. Pollard, and J. T. Allen (2006), Large-scale physical controls on phytoplankton growth in the Irminger Sea Part I: Hydrographic zones, mixing and stratification, *J. Mar. Syst.*, *59*(3–4), 201–218, doi:10.1016/j.jmarsys.2005.10.004.

Holliday, N. P., A. Meyer, S. Bacon, S. G. Alderson, and B. de Cuevas (2007), Retroflection of part of the east Greenland current at Cape Farewell, *Geophys. Res. Lett.*, *34*, L07609, doi:10.1029/2006GL029085.

Holliday, N. P., S. Bacon, J. Allen, and E. L. McDonagh (2009), Circulation and transport in the western boundary currents at Cape Farewell, Greenland, *J. Phys. Oceanogr.*, *39*(8), 1854–1870, doi:10.1175/2009JPO4160.1.

Hunter, S., D. Wilkinson, E. Louarn, I. Nick McCave, E. Rohling, D. A. V. Stow, and S. Bacon (2007a), Deep western boundary current dynamics and associated sedimentation on the Eirik Drift, Southern Greenland Margin, *Deep-Sea Res. Part Oceanogr. Res. Pap.*, *54*(12), 2036–2066, doi:10.1016/j.dsr.2007.09.007.

Hunter, S. E., D. Wilkinson, J. Stanford, D. A. V. Stow, S. Bacon, A. M. Akhmetzhanov, and N. H. Kenyon (2007b), The Eirik Drift: A long-term barometer of North Atlantic deepwater flux south of Cape Farewell, Greenland, *Geol. Soc. London Spec. Publ.*, *276*, 245–263, doi:10.1144/GSL.SP.2007.276.01.12.

Hurrell, J. W. (1995), Decadal trends in the North Atlantic oscillation: Regional temperatures and precipitation, *Science*, *269*(5224), 676–679, doi:10.1126/science.269.5224.676.

Ineson, S., and A. A. Scaife (2009), The role of the stratosphere in the European climate response to El Niño, *Nat. Geosci.*, *2*(1), 32–36, doi:10.1038/ngeo381.

International Panel on Climate Change (2007), *Climate Change 2007: The Physical Sciene Basis*, Cambridge Univ. Press, Cambridge, England.

Irvali, N., U. S. Ninnemann, E. V. Galaasen, Y. Rosenthal, D. Kroon, D. W. Oppo, H. F. Kleiven, K. F. Darling, and C. Kissel (2012), Rapid switches in subpolar North Atlantic hydrography and climate during the Last Interglacial (MIS 5e), *Paleoceanography*, *27*, PA2207, doi:10.1029/2011PA002244.

Jennings, A. E., and N. J. Weiner (1996), Environmental change in eastern Greenland during the last 1300 years: Evidence from foraminifera and lithofacies in Nansen Fjord, 68°N, *Holocene*, *6*(2), 179–191, doi:10.1177/095968369600600205.

Jiang, H., J. Eiríksson, M. Schulz, K. L. Knudsen, and M. S. Seidenkrantz (2005), Evidence for solar forcing of sea-surface temperature on the North Icelandic Shelf during the late Holocene, *Geology*, *33*(1), 73–76, doi:10.1130/G21130.1.

Jonkers, L., G. J. A. Brummer, F. J. C. Peeters, H. M. Van Aken, and M. F. De Jong (2010), Seasonal stratification, shell flux, and oxygen isotope dynamics of leftcoiling N. pachyderma and T. quinqueloba in the western subpolar North Atlantic, *Paleoceanography*, *25*, PA2204, doi:10.1029/2009PA001849.

Kaufman, D. S., et al. (2009), Recent warming reverses long-term arctic cooling, *Science*, *325*(5945), 1236–1239, doi:10.1126/science.1173983.

Keigwin, L. D. (1996), The Little Ice Age and Medieval Warm Period in the Sargasso Sea, *Science*, *274*(5292), 1504–1508, doi:10.1126/science.274.5292.1503.

Key, R. M., A. Kozyr, C. L. Sabine, K. Lee, R. Wanninkhof, J. L. Bullister, R. A. Feely, F. J. Millero, C. Mordy, and T. H. Peng (2004), A global ocean carbon climatology: Results from Global Data Analysis Project (GLODAP), *Global Biogeochem. Cycles*, *18*, GB4031, doi:10.1029/2004GB002247.

Kleiven, H. F., C. Kissel, C. Laj, U. S. Ninnemann, T. O. Richter, and E. Cortijo (2008), Reduced North Atlantic Deep Water coeval with the glacial Lake Agassiz freshwater outburst, *Science*, *319*(5859), 60–64, doi:10.1126/science.1148924.

Koch, L. (1945), The east Greenland ice, *Medd Grønl. Kbh.*, *130*(3), 1–374.

Kohfeld, K. E., R. G. Fairbanks, S. L. Smith, and I. D. Walsh (1996), Neogloboquadrina pachyderma (sinistral coiling) as paleoceanographic tracers in polar oceans: Evidence from Northeast Water Polynya plankton tows, sediment traps, and surface sediments, *Paleoceanography*, *11*(6), 679–699, doi:10.1029/96PA02617.

Kozdon, R., T. Ushikubo, N. T. Kita, M. Spicuzza, and J. W. Valley (2009a), Intratest oxygen isotope variability in the planktonic foraminifer N. pachyderma: Real vs. apparent vital effects by ion microprobe, *Chem. Geol.*, *258*(3–4), 327–337, doi:10.1016/j.chemgeo.2008.10.032.

Kozdon, R., A. Eisenhauer, M. Weinelt, M. Y. Meland, and D. Nürnberg (2009b), Reassessing Mg/Ca temperature calibrations of Neogloboquadrina pachyderma (sinistral) using paired δ44/40Ca and Mg/Ca measurements, *Geochem. Geophys. Geosyst.*, *10*, Q03005, doi:10.1029/2008GC002169.

Kreutz, K. J., P. A. Mayewski, L. D. Meeker, M. S. Twickler, S. I. Whitlow, and I. I. Pittalwala (1997), Bipolar changes in atmospheric circulation during the Little Ice Age, *Science*, *277*(5330), 1294–1296, doi:10.1126/science.277.5330.1294.

Kucera, M. (2007), Chapter six planktonic foraminifera as tracers of past oceanic environments, in *Developments in Marine Geology*, vol. 1, edited by H. Claude and A. De Vernal, pp. 213–262, Elsevier, Amsterdam.

Kucera, M., et al. (2005), Reconstruction of sea-surface temperatures from assemblages of planktonic foraminifera: Multi-technique approach based on geographically constrained calibration data sets and its application to glacial Atlantic and Pacific Oceans, *Quat. Sci. Rev.*, *24*(7–9), 951–998, doi:10.1016/j.quascirev.2004.07.014.

Kuhlbrodt, T., A. Griesel, M. Montoya, A. Levermann, M. Hofmann, and S. Rahmstorf (2007), On the driving processes of the Atlantic meridional overturning circulation, *Rev. Geophys.*, *45*, RG2001, doi:10.1029/2004RG000166.

Lamb, H. H. (1965), The early medieval warm epoch and its sequel, *Palaeogeogr. Palaeoclimatol. Palaeoecol.*, *1*(0), 13–37, doi:10.1016/0031-0182(65)90004-0.

Lavender, K. L., W. Brechner Owens, and R. E. Davis (2005), The mid-depth circulation of the subpolar North Atlantic Ocean as measured by subsurface floats, *Deep-Sea Res. Part Oceanogr. Res. Pap.*, *52*(5), 767–785, doi:10.1016/j.dsr.2004.12.007.

Lazier, J. R. N. (1980), Oceanographic conditions at Ocean Weather Ship Bravo, 1964–1974, *Atmos.–#cean*, *18*(3), 227–238, doi:10.1080/07055900.1980.9649089.

Lazier, J., R. Hendry, A. Clarke, I. Yashayaev, and P. Rhines (2002), Convection and restratification in the Labrador Sea, 1990–2000, *Deep-Sea Res. Part Oceanogr. Res. Pap.*, *49*(10), 1819–1835, doi:10.1016/S0967-0637(02)00064-X.

LeGrande, A. N., and G. A. Schmidt (2006), Global gridded data set of the oxygen isotopic composition in seawater, *Geophys. Res. Lett.*, *33*, L12604, doi:10.1029/2006GL026011.

Lehner, F., C. C. Raible, and T. F. Stocker (2012), Testing the robustness of a precipitation proxy-based North Atlantic Oscillation reconstruction, *Quat. Sci. Rev.*, *45*(0), 85–94, doi:10.1016/j.quascirev.2012.04.025.

Lehner, F., A. Born, C. C. Raible, and T. F. Stocker (2013), Amplified inception of European Little Ice Age by sea ice–ocean–atmosphere feedbacks, *J. Clim.*, *26*(19), 7586–7602, doi:10.1175/JCLI-D-12-00690.1.

Lockwood, M., R. G. Harrison, T. Woollings, and S. K. Solanki (2010), Are cold winters in Europe associated with low solar activity?, *Environ. Res. Lett.*, *5*(2), 024001, doi:10.1088/1748-9326/5/2/024001.

Lu, Y., D. G. Wright, and I. Yashayaev (2007), Modelling hydrographic changes in the Labrador Sea over the past five decades, *Prog. Oceanogr.*, *73*(3–4), 406–426, doi:10.1016/j.pocean.2007.02.007.

Luo, H., A. Bracco, I. Yashayaev, and E. Di Lorenzo (2012), The interannual variability of potential temperature in the central Labrador Sea, *J. Geophys. Res.*, *117*, C10016, doi:10.1029/2012JC007988.

Mann, M. E., M. A. Cane, S. E. Zebiak, and A. Clement (2005), Volcanic and solar forcing of the tropical Pacific over the past 1000 years, *J. Clim.*, *18*(3), 447–456, doi:10.1175/jcli-3276.1.

Mann, M. E., Z. Zhang, S. Rutherford, R. S. Bradley, M. K. Hughes, D. Shindell, C. Ammann, G. Faluvegi, and F. Ni (2009), Global signatures and dynamical origins of the Little Ice Age and Medieval Climate Anomaly, *Science*, *326*(5957), 1256–1260, doi:10.1126/science.1177303.

Marshall, J., and F. Schott (1999), Open-ocean convection: Observations, theory, and models, *Rev. Geophys.*, *37*(1), 1–64, doi:10.1029/98RG02739.

Massé, G., S. J. Rowland, M. A. Sicre, J. Jacob, E. Jansen, and S. T. Belt (2008), Abrupt climate changes for Iceland during the last millennium: Evidence from high resolution sea ice reconstructions, *Earth Planet. Sci. Lett.*, *269*(3–4), 564–568, doi:10.1016/j.epsl.2008.03.017.

Mayewski, P. A., L. D. Meeker, M. S. Twickler, S. Whitlow, Y. Qinzhao, W. Berry Lyons, and M. Prentice (1997), Major features and forcing of high-latitude Northern Hemisphere atmospheric circulation using a 110 000-year-long glaciochemical series, *J. Geophys. Res.*, *102*(C12), 26,345–26,366, doi:10.1029/96JC03365.

Meeker, L. D., and P. A. Mayewski (2002), A 1400-year high-resolution record of atmospheric circulation over the North Atlantic and Asia, *Holocene*, *12*(3), 257–266, doi:10.1191/0959683602hl542ft.

Mignot, J., M. Khodri, C. Frankignoul, and J. Servonnat (2011), Volcanic impact on the Atlantic Ocean over the last millennium, *Clim. Past*, *7*(4), 1439–1455, doi:10.5194/cp-7-1439-2011.

Miller, G. H., et al. (2012), Abrupt onset of the Little Ice Age triggered by volcanism and sustained by sea-ice/ocean feedbacks, *Geophys. Res. Lett.*, *39*, L02708, doi:10.1029/2011GL050168.

Moffa-Sanchez, P., A. Born, I. R. Hall, and D. J. R. Thornalley (2014), Solar forcing of North Atlantic surface temperature and salinity over the last millennium, *Nat. Geosci.*, *7*, doi:10.1038/ngeo2094.

Moreno, A., et al. (2012), The Medieval Climate Anomaly in the Iberian Peninsula reconstructed from marine and lake records, *Quat. Sci. Rev.*, *43*(0), 16–32, doi:10.1016/j.quascirev.2012.04.007.

Morey, A. E., A. C. Mix, and N. G. Pisias (2005), Planktonic foraminiferal assemblages preserved in surface sediments correspond to multiple environment variables, *Quat. Sci. Rev.*, *24*(7–9), 925–950, doi:10.1016/j.quascirev.2003.09.011.

Moros, M., J. T. Andrews, D. D. Eberl, and E. Jansen (2006), Holocene history of drift ice in the northern North Atlantic: Evidence for different spatial and temporal modes, *Paleoceanography*, *21*, PA2017, doi:10.1029/2005PA001214.

Mulitza, S., A. Dürkoop, W. Hale, G. Wefer, and H. S. Niebler (1997), Planktonic foraminifera as recorders of past surface-water stratification, *Geology*, *25*(4), 335–338, doi:10.1130/0091-7613(1997)025.

Nesje, A., J. Bakke, S. O. Dahl, Ø. Lie, and J. A. Matthews (2008), Norwegian mountain glaciers in the past, present and future, *Hist. Holocene Glacier – Clim. Var.*, *60*(1–2), 10–27, doi:10.1016/j.gloplacha.2006.08.004.

Nyland, B. F., E. Jansen, H. Elderfield, and C. Andersson (2006), Neogloboquadrina pachyderma (dex. and sin.) Mg/Ca and δ18O records from the Norwegian Sea, *Geochem. Geophys. Geosyst.*, *7*, Q10P17, doi:10.1029/2005GC001055.

Ogilvie, A. E. J., and T. Jónsson (2001), Little Ice Age" research: A perspective from Iceland, *Clim. Change*, *48*, 9–52, doi:10.1023/A:1005625729889.

Olsen, J., N. J. Anderson, and M. F. Knudsen (2012), Variability of the North Atlantic Oscillation over the past 5,200 years, *Nat. Geosci.*, *5*(11), 808–812, doi:10.1038/ngeo1589.

Parnell, A. C., C. E. Buck, and T. K. Doan (2011), A review of statistical chronology models for high-resolution, proxy-based Holocene palaeoenvironmental reconstruction, *Quat. Sci. Rev.*, *30*(21–22), 2948–2960, doi:10.1016/j.quascirev.2011.07.024.

Perner, K., M. Moros, J. M. Lloyd, A. Kuijpers, R. J. Telford, and J. Harff (2011), Centennial scale benthic foraminiferal record of late Holocene oceanographic variability in Disko Bugt, West Greenland, *Quat. Sci. Rev.*, *30*(19–20), 2815–2826, doi:10.1016/j.quascirev.2011.06.018.

Price, J. F., and M. O. Baringer (1994), Outflows and deep-water production by marginal seas, *Prog. Oceanogr.*, *33*(3), 161–200, doi:10.1016/0079-6611(94)90027-2.

Proctor, C. J., A. Baker, W. L. Barnes, and M. A. Gilmour (2000), A thousand year speleothem proxy record of North Atlantic climate from Scotland, *Clim. Dyn.*, *16*(10–11), 815–820, doi:10.1007/s003820000077.

Raible, C., M. Yoshimori, T. Stocker, and C. Casty (2007), Extreme midlatitude cyclones and their implications for precipitation and wind speed extremes in simulations of the Maunder Minimum versus present day conditions, *Clim. Dyn.*, *28*(4), 409–423, doi:10.1007/s00382-006-0188-7.

Rashid, H., and E. A. Boyle (2007), Mixed-layer deepening during Heinrich events: A multi-planktonic foraminiferal δ18O approach, *Science*, *318*(5849), 439–441, doi:10.1126/science.1146138.

Reimer, P. J., et al. (2009), *IntCal09 And Marine09 Radiocarbon Age Calibration Curves, 0–50,000 Years Cal BP*, University of Arizona, Tucson, AZ, ETATS-UNIS.

Rhein, M., J. Fischer, W. M. Smethie, D. Smythe-Wright, R. F. Weiss, C. Mertens, D. H. Min, U. Fleischmann, and A. Putzka (2002), Labrador Sea Water: Pathways, CFC inventory, and formation rates, *J. Phys. Oceanogr.*, *32*(2), 648–665, doi:10.1175/1520-0485(2002)032.

Richter, T. O., F. J. C. Peeters, and T. C. E. van Weering (2009), Late Holocene (0–2.4 ka BP) surface water temperature and salinity variability, Feni Drift, NE Atlantic Ocean, *Quat. Sci. Rev.*, *28*(19–20), 1941–1955, doi:10.1016/j.quascirev.2009.04.008.

Robock, A. (2000), Volcanic eruptions and climate, *Rev. Geophys.*, *38*(2), 191–219.

Rodwell, M. J., D. P. Rowell, and C. K. Folland (1999), Oceanic forcing of the wintertime North Atlantic Oscillation and European climate, *Nature*, *398*(6725), 320–323, doi:10.1038/18648.

Scaife, A. A., S. Ineson, J. R. Knight, L. Gray, K. Kodera, and D. M. Smith (2013), A mechanism for lagged North Atlantic climate response to solar variability, *Geophys. Res. Lett.*, *40*, 434–439, doi:10.1002/grl.50099.

Schmidt, G. A. (1999), Error analysis of paleosalinity calculations, *Paleoceanography*, *14*(3), 422–429, doi:10.1029/1999PA900008.

Schneider, D. P., C. M. Ammann, B. L. Otto-Bliesner, and D. S. Kaufman (2009), Climate response to large, high-latitude and low-latitude volcanic eruptions in the community climate system model, *J. Geophys. Res.*, *114*, D15101, doi:10.1029/2008JD011222.

Sedláček, J., and L. Mysak (2009a), A model study of the Little Ice Age and beyond: Changes in ocean heat content, hydrography and circulation since 1500, *Clim. Dyn.*, *33*(4), 461–475, doi:10.1007/s00382-008-0503-6.

Sedláček, J., and L. Mysak (2009b), Sensitivity of sea ice to wind-stress and radiative forcing since 1500: A model study of the Little Ice Age and beyond, *Clim. Dyn.*, *32*(6), 817–831, doi:10.1007/s00382-008-0406-6.

Shackleton, N. J. (1974), Attainment of isotopic equilibrium between ocean water and the benthonic foraminifera genus Uvigerina: Isotopic changes in the ocean during the last glacial, *Cent. Nat. Rech. Sci. Colloq. Int.*, *219*, 203–209.

Shindell, D. T., G. A. Schmidt, M. E. Mann, D. Rind, and A. Waple (2001), Solar forcing of regional climate change during the Maunder Minimum, *Science*, *294*(5549), 2149–2152, doi:10.1126/science.1064363.

Sicre, M. A., J. Jacob, U. Ezat, S. Rousse, C. Kissel, P. Yiou, J. Eiríksson, K. L. Knudsen, E. Jansen, and J. L. Turon (2008), Decadal variability of sea surface temperatures off North Iceland over the last 2000 years, *Earth Planet. Sci. Lett.*, *268*(1–2), 137–142, doi:10.1016/j.epsl.2008.01.011.

Sicre, M. A., I. R. Hall, J. Mignot, M. Khodri, U. Ezat, M. X. Truong, J. Eiríksson, and K. L. Knudsen (2011), Sea surface temperature variability in the subpolar Atlantic over the last two millennia, *Paleoceanography*, *26*, PA4218, doi:10.1029/2011PA002169.

Simstich, J., M. Sarnthein, and H. Erlenkeuser (2003), Paired δ18O signals of Neogloboquadrina pachyderma(s) and Turborotalita quinqueloba show thermal stratification structure in Nordic Seas, *Mar. Micropaleontol.*, *48*(1–2), 107–125, doi:10.1016/S0377-8398(02)00165-2.

Spangehl, T., U. Cubasch, C. C. Raible, S. Schimanke, J. Körper, and D. Hofer (2010), Transient climate simulations from the Maunder Minimum to present day: Role of the stratosphere, *J. Geophys. Res.*, *115*, D00I10, doi:10.1029/2009JD012358.

Stangeew, E. (2001), Distribution and isotopic composition of living planktonic foraminifera N. pachyderma (sinistral) and T. quinqueloba in the high latitude North Atlantic, Christian-Albrechts-Univ., Kiel, Germany.

Steinhilber, F., J. Beer, and C. Fröhlich (2009), Total solar irradiance during the Holocene, *Geophys. Res. Lett.*, *36*, L19704, doi:10.1029/2009GL040142.

Straneo, F. (2006), Heat and freshwater transport through the central Labrador Sea, *J. Phys. Oceanogr.*, *36*(4), 606–628, doi:10.1175/JPO2875.1.

Swingedouw, D., L. Terray, C. Cassou, A. Voldoire, D. Salas-Melia, and J. Servonnat (2011), Natural forcing of climate during the last millennium: Fingerprint of solar variability, *Clim. Dyn.*, *36*(7–8), 1349–1364, doi:10.1007/s00382-010-0803-5.

Talley, L. D. (2003), Shallow, intermediate, and deep overturning components of the global heat budget, *J. Phys. Oceanogr.*, *33*(3), 530–560, doi:10.1175/1520-0485(2003)033.

Talley, L. D., and M. S. McCartney (1982), Distribution and circulation of Labrador Sea Water, *J. Phys. Oceanogr.*, *12*, 1189–1205, doi:10.1175/1520-0485(1982)012.

Thornalley, D. J. R., H. Elderfield, and I. N. McCave (2009), Holocene oscillations in temperature and salinity of the surface subpolar North Atlantic, *Nature*, *457*(7230), 711–714, doi:10.1038/nature07717.

Tolderlund, D. S., and A. W. H. Be (1971), Seasonal distribution of planktonic foraminifera in the western North Atlantic, *Micropaleontol. N. Y.*, *17*(3), 297–329, doi:10.2307/1485143.

Trouet, V., J. Esper, N. E. Graham, A. Baker, J. D. Scourse, and D. C. Frank (2009), Persistent positive north atlantic oscillation mode dominated the medieval climate anomaly, *Science*, *324*(5923), 78–80, doi:10.1126/science.1166349.

Trouet, V., J. D. Scourse, and C. C. Raible (2012), North Atlantic storminess and Atlantic Meridional Overturning Circulation during the last Millennium: Reconciling contradictory proxy records of NAO variability, *Global Planet. Change*, *84–85*, 48–55, doi:10.1016/j.gloplacha.2011.10.003.

Walsh, J. E., and W. L. Chapman (1990), Arctic contribution to upper-ocean variability in the North Atlantic, *J. Clim.*, *3*(12), 1462–1473, doi:10.1175/1520-0442(1990)0032.0.CO;2.

Wanamaker, A. D., P. G. Butler, J. D. Scourse, J. Heinemeier, J. Eiríksson, K. L. Knudsen, and C. A. Richardson (2012), Surface changes in the North Atlantic meridional overturning circulation during the last millennium, *Nat. Commun.*, *3*, 899, doi:10.1038/ncomms1901.

Wassenburg, J. A., et al. (2013), Moroccan speleothem and tree ring records suggest a variable positive state of the North Atlantic Oscillation during the Medieval Warm Period, *Earth Planet. Sci. Lett.*, *375*(0), 291–302, doi:10.1016/j.epsl.2013.05.048.

Wintle, A. G., M. L. Clarke, F. M. Musson, J. D. Orford, and R. J. N. Devoy (1998), Luminescence dating of recent dunes on Inch Spit, Dingle Bay, southwest Ireland, *Holocene*, *8*(3), 331–339, doi:10.1191/095968398671791976.

Woollings, T., M. Lockwood, G. Masato, C. Bell, and L. Gray (2010), Enhanced signature of solar variability in Eurasian winter climate, *Geophys. Res. Lett.*, *37*, L20805, doi:10.1029/2010GL044601.

Yashayaev, I. (2007a), Hydrographic changes in the Labrador Sea, 1960–2005, *Prog. Oceanogr.*, *73*(3–4), 242–276, doi:10.1016/j.pocean.2007.04.015.

Yashayaev, I. (2007b), Changing freshwater content: Insights from the subpolar North Atlantic and new oceanographic challenges, *Prog. Oceanogr.*, *73*(3–4), 203–209, doi:10.1016/j.pocean.2007.04.014.

Yashayaev, I., N. P. Holliday, M. Bersch, and H. Aken (2008), The history of the Labrador Sea Water: Production, spreading, transformation and loss, in *Arctic–Subarctic Ocean Fluxes*, edited by R. Dickson, J. Meincke, and P. Rhines, pp. 569–612, Springer, Netherlands.

Yashayaev, I., and J. W. Loder (2009), Enhanced production of Labrador Sea Water in 2008, *Geophys. Res. Lett.*, *36*, L01606, doi:10.1029/2008GL036162.

Zhong, Y., G. H. Miller, B. L. Otto-Bliesner, M. M. Holland, D. A. Bailey, D. P. Schneider, and A. Geirsdottir (2011), Centennial-scale climate change from decadally-paced explosive volcanism: A coupled sea ice-ocean mechanism, *Clim. Dyn.*, *37*(11–12), 2373–2387, doi:10.1007/s00382-010-0967-z.

Zorita, E., H. Von Storch, F. J. Gonzalez-Rouco, U. Cubasch, J. Luterbacher, S. Legutke, I. Fischer-Bruns, and U. Schlese (2004), Climate evolution in the last five centuries simulated by an atmosphere–ocean model: Global temperatures, the North Atlantic Oscillation and the Late Maunder Minimum, *Meteorol. Z.*, *13*, 271–289, doi:10.1127/0941-2948/2004/0013-0271.